MATHEMATICAL MODEL AND ANALYTICAL SOLUTION FOR THE VIBRATION OF INCLINED FLUID-TRANSPORTING SUBMARINE PIPELINES

(DOI No: 10.3940/rina.ijme.2019.a4.524)

C An*, **T T Li**, **W Liang** and **M L Duan**, College of Safety and Ocean Engineering, China University of Petroleum-Beijing, China, **H B Huang** School of Geography, University College Cork, Ireland

SUMMARY

Due to the complexity of submarine environments, the nature of the dynamic response of free-spanning submarine pipelines, particularly inclined pipelines, is unclear. This paper aims to theoretically analyze the vibration behaviors of inclined fluid-transporting free-spanning submarine pipelines in the deepwater area. The mathematical model for the vibration of inclined fluid-transporting pipelines is established considering the influence of gravity on vibration response, and a non-linear wake oscillator is employed to model the vortex shedding behind the pipeline free span. The partial differential equation system is solved through the generalized integral transform technique (GITT), which is an analytical or semi-analytical method. Parametric analysis are carried out to investigate the effects of the inclination on the dynamic response of fluid-transporting pipelines. It is found that the inclination of the free-spanning pipeline will radically alter the natural frequency of the structure, and consequently the VIV lock-in region. In addition, the slope of the seabed will cause a more significant internal flow effect. The thorough theoretical understanding of inclined fluid-transporting pipelines helps increase the design accuracy for pipelines installed on a seabed with a highly irregular topography.

1. INTRODUCTION

As a transportation facility in offshore engineering, the submarine pipeline plays a crucial role in transporting oil and gas from deep down the bottom of the sea to the far away user terminal. Deep and even ultra-deep water create a wide range of challenges for pipeline design in oil and gas industry and the safety operation of pipelines must be prioritized considering their importance and coverage in any oil and gas projects, particularly the offshore projects.

In deepwater area, pipelines are laid on the seabed and due to scour of the current or seabed unevenness, some parts of submarine pipelines may have to cross a depression or a gully (Fyrileiv & Mørk, 2002), and the pipeline section between two touchdown points is called a free span (Vedeld, et al, 2013). If a free-span is exposed to currents, vortex shedding may occur and produce vibration of the pipeline structure. The vortex-induced vibration (VIV) of the suspended part of the pipeline may consequently induce accumulative fatigue damage of the pipelines. This consequence is one of the most concerned issues in the design of submarine pipelines.

Due to its simplicity and effectiveness, the wake oscillator model has been acknowledged as a feasible way to model the vortex shedding. Facchinetti et al. (2004) investigated three different coupling terms, i.e. acceleration, velocity and displacement to study the VIV of pipelines, and concluded that the acceleration coupling best coincide with the experimental results. Low and Srinil (2016) carried out a nonlinear fluid-structure interaction analysis of marine risers by identifying the uncertainties of a wake oscillator model which simulates the fluctuating hydrodynamic force. However, the above-mentioned literature neglect the fact that pipelines and risers in offshore engineering often transport fluid. For pipelines that transport internal fluid, the dynamic behaviors are affected by both the current and fluid running inside itself. The currents and the pipelines transporting internal fluid interact with each other and form a coupled nonlinear system. The pipelines exposed to currents are prone to VIV, while the internal fluid travels along the curved pipeline amplifies the vibration of the system to an extent that the effect cannot be neglected when predicting the fatigue life of submarine pipelines (Guo, et al, 2006).

Housner (1952) is one of the pioneers who studied the dynamic behaviors of pipelines considering the effect of internal fluid in pipelines and showed that at certain high velocity, the internal fluid will even cause dynamic instability of the pipeline. Based on Housner's model, Shen and Zhao (1996) studied the impact of internal fluid on the fatigue life of the pipeline free span subject to VIV. Guo et al. (2004), Lou et al. (2005) and Guo and Lou (2008) investigated the coupled effect of internal and external fluid on the vibration behavior of free-spanning pipelines by using Finite Element Method (FEM). Kaewunruen et al. (2005) investigated nonlinear free vibrations of marine pipes transporting fluid, and determined the nonlinear fundamental frequencies and the mode shapes by the modified direct iteration technique. And lately, Dai et al. (2014) investigated the VIV of pipes conveying pulsating fluid through the direct perturbation method of multiple scales.

It should be noted that the majority of the previous literature on this topic consider the pipelines in the horizontal position and neglect the fact that in real circumstances, pipelines are most likely to be placed over

a slope. For instance, it is reported that the maximum slope is about 22° for the Southern Route, and 25° for the Northern Route of the pipeline Transmed stretching from Algeria to Italy (Drago, et al, 2015). Paidoussis (1998) pointed out that for vertical pipelines vibrating freely, the effect of gravity is non-negligible, suggesting that the influence of gravity is important on the dynamic response of inclined pipelines and thus should be considered. Gan et al. (2015) and Jing et al. (2015) built a mathematical model to study the vibration behavior of an inclined viscoelastic pipe. Results show that the vibration of inclined fluid-conveying pipes demonstrates bifurcation processes. However, in their model, only the internal fluid was considered.

In this work, considering the effect of gravity, a fluid-structural model is proposed to analyze the dynamic behavior of inclined submarine pipelines subjected to internal flow and external current. A thorough understanding of their dynamic behaviors will help the design of pipelines. In Section 2, the governing equation for the vibration of inclined submarine fluid-transporting pipelines is established, and a non-linear wake oscillator is employed to model the vortex shedding behind the pipeline. Section 3 provides the analytical or semi-analytical solutions for the transverse displacement using the generalized integral transform technique (GITT). Case studies, presented in Section 4, include the structural natural frequency, mode shapes, and effect analysis of the inclination and internal fluid on the dynamic response through time history, and frequency analyses. The final results and discussions are concluded in Section 5 of the paper.

2. MATHEMATICAL MODEL

Consider a Cartesian coordinate system of *x'*- and *z'*-axes, with its origin at the left end of the pipeline, where *x'*-axis is in the direction of the gravity. Being rotated counter-clockwise by θ, a new coordinate system of *x*-, *y*- and *z*-axes is sketched, where the *y*-axis is parallel to the current and orthogonal to *x*- and *z*-axes, and *z*-is the direction along which the pipeline deflects transversely. Taking the free-spanning submarine pipeline as an example, the diagram is illustrated in Figure 1.

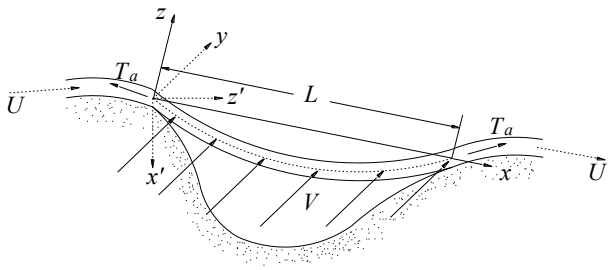

Figure 1: Schematic diagram of a fluid-conveying free-spanning submarine pipeline over a slope.

In the present study, the pipeline is assumed to be elastic, non-deformed, and simple-supported at both ends. The internal fluid inside the pipe travels at a constant velocity *U*, and the external current flows at a constant velocity *V*. The pipeline is cylindrical with a constant outer diameter *D* and inner diameter D_i. Its outer cross section area is symbolized as A_e, the inner cross section area A_i, and the inner perimeter is S_i. The axial tension and internal pressure are T_a and *P*, respectively. This model is constrained to cross-flow vibration.

2.1 STRUCTURE MODEL

The forces and moments acting on the fluid and pipe elements δx are analyzed respectively as Figure 2 shows. The internal fluid is assumed to be steady and incompressible. Since the diameter of the pipe is small compared with the wavelength of the disturbances to the fluid particle, its accelerations in *x*- and *z*-directions are respectively zero and $\left(\frac{\partial}{\partial t}+U\frac{\partial}{\partial x}\right)^2 z$.

τ stands for the shear force acting on the inner surface of the pipeline, hence τS_i represents the friction between the internal fluid and the inner surface. *f* is the transverse force between the pipe and the internal fluid. r_s is the structural damping. *g* is the acceleration due to the gravity. For unit length of the pipeline, m_i is the internal fluid mass, m_p is the mass of the pipeline, and $m_e = C_M \pi \rho_e D^2/4$ is the added mass due to external fluid, where C_M is the added mass coefficient. The density of the pipe, the internal fluid and the external current are expressed respectively as ρ_p, ρ_i and ρ_e. *Q* is the transverse shear force on the pipe element, and *M* is the bending moment. F_w is the force due to the current in the cross-flow direction, expressed as $F_w = F_L + \rho_e g A_e \sin\theta - r_f \frac{\partial z}{\partial t} - m_e \frac{\partial^2 z}{\partial t^2}$, where $F_L = \frac{C_L \rho_e V^2 D}{2}$ is the lift force, and $r_f = \lambda \Omega_f \rho_e D^2$ is the external fluid added damping, with λ being related to the drag mean sectional drag coefficient of the structure C_D through $\lambda = C_D/(4\pi St)$.

By neglecting the terms of second or higher order, according to the Euler beam approximation for small deformation, the force equilibrium equations are as follows:

$$-A_i \frac{\partial P}{\partial x} - \tau S_i + m_i g \sin\theta + f\frac{\partial z}{\partial x} - m_i \frac{\partial U}{\partial t} = 0 \quad \text{(in } x\text{-direction)} \tag{1a}$$

and

$$f + m_i g \sin\theta + A_i \frac{\partial P}{\partial x}\frac{\partial z}{\partial x} + A_i P \frac{\partial^2 z}{\partial x^2} + \tau S_i \frac{\partial z}{\partial x} + m_i (\frac{\partial}{\partial t} + U\frac{\partial}{\partial x})^2 z = 0$$

(in *z*-direction) (1b)

In terms of the pipe element, similarly, the force equilibrium equations are concluded as follows:

$$\frac{\partial T_a}{\partial x} + \tau S_i + m_p g \cos\theta - f\frac{\partial z}{\partial x} = 0$$

(in *x*-direction) (2a)

and

$$\frac{\partial Q}{\partial x} + T_a \frac{\partial^2 z}{\partial x^2} + \frac{\partial T_a}{\partial x}\frac{\partial z}{\partial x} + f - m_p g \sin\theta + \tau S_i \frac{\partial z}{\partial x} - r_s \frac{\partial z}{\partial t} - m_p \frac{\partial^2 z}{\partial t^2} + F_w = 0$$

(in z-direction) (2b)

Considering $Q = -\frac{\partial M}{\partial x} = -EI\frac{\partial^3 z}{\partial x^3}$, where *EI* is the flexural stiffness, the governing equation for the vibration of inclined fluid-transporting submarine pipelines is derived based on Equations (1) and (2):

$$EI\frac{\partial^4 z}{\partial x^4} + (m_i U^2 + PA_i - T_a)\frac{\partial^2 z}{\partial x^2} + (m_p + m_i)g\cos\theta\frac{\partial z}{\partial x} + 2m_i U\frac{\partial^2 z}{\partial x \partial t} + (r_s + r_f)\frac{\partial z}{\partial t} + (m_p + m_i + m_e)\frac{\partial^2 z}{\partial t^2} + (m_p + m_i)g\sin\theta - \rho_e g A_e \sin\theta = F_L \quad (3)$$

According to Facchinetti el al. (2004), the structural damping can be calculated by $r_s = 2m\Omega_s\zeta$, where ζ is the damping ratio, and Ω_s is the angular structural natural frequency. For a simple-supported beam, it can be calculated through $\Omega_s = \pi^2\sqrt{\frac{EI}{mL^4}}$ (Clough & Penzien, 1975).

2.2 WAKE OSCILLATOR MODEL

In the present paper, a nonlinear oscillator equation is adopted to describe the fluid force acted on the structure by the current (Facchinetti, et al, 2004; Iwan, 1981), which is expressed as follows:

$$\frac{\partial^2 q}{\partial t^2} + \varepsilon\Omega_f (q^2 - 1)\frac{\partial q}{\partial t} + \Omega_f{}^2 q = F \quad (4)$$

The dimensionless wake variable *q* (as shown in Figure 3) is related to the fluctuating lift coefficient C_L on the structure, i.e. $q(x,t) = 2C_L(x,t)/C_{L0}$, where C_{L0} is the reference lift coefficient which can be obtained from experiments. On the right-hand side of Equation (4), the forcing term $F = \frac{a}{D}\frac{\partial^2 z}{\partial t^2}$ simulates the effects of the pipe motion on the near wake. $\Omega_f = 2\pi StV/D$ denotes the vortex-shedding angular frequency, where *St* is the Strouhal number. The values of the van der Pol parameter ε and the coupling force scaling parameter *A* can also be gained through experiments.

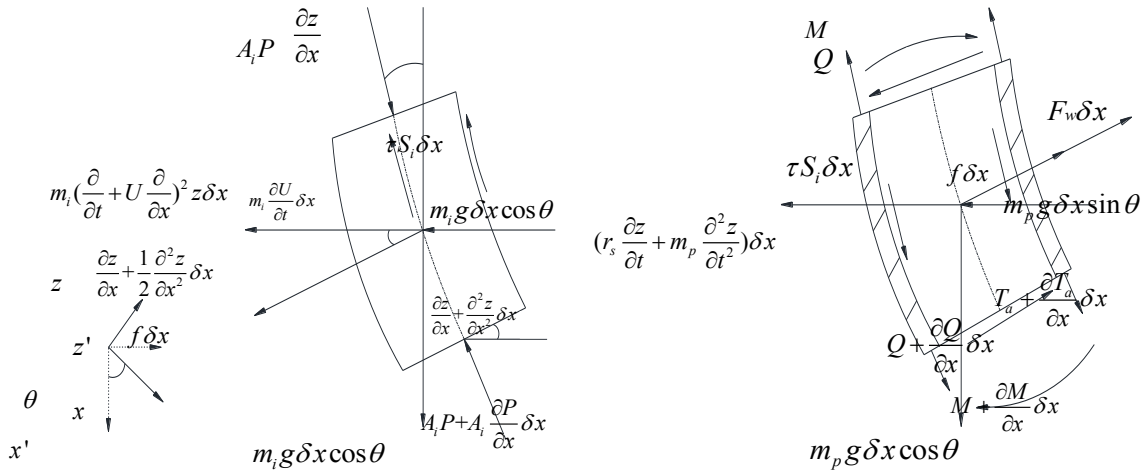

(a) Fluid element (b) Pipe element

Figure 2: Forces and moments acting on the elements.

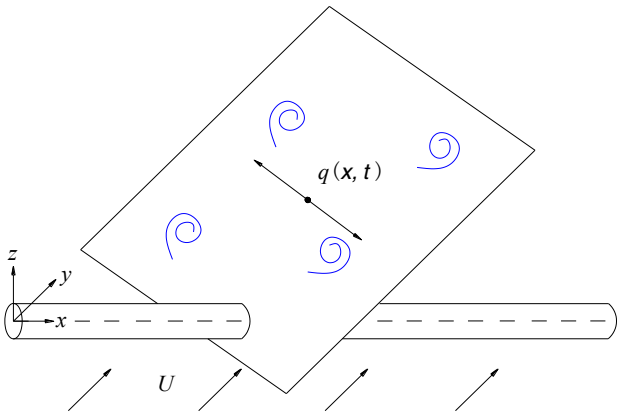

Figure 3: Wake oscillators for cross-flow vibration.

2.3 COUPLING OF STRUCTURE AND WAKE MODELS

By combining Equations (3) and (4), the following coupled fluid-structure dynamic system is derived:

$$\begin{cases} EI\dfrac{\partial^4 z}{\partial x^4}+(m_i U^2+PA_i-T_a)\dfrac{\partial^2 z}{\partial x^2}+(m_p+m_i)g\cos\theta\dfrac{\partial z}{\partial x}+2m_i U\dfrac{\partial^2 z}{\partial x\partial t}+(r_s+r_f)\dfrac{\partial z}{\partial t}+(m_p+m_i+m_e)\dfrac{\partial^2 z}{\partial t^2} \\ +(m_p+m_i)g\sin\theta-\rho_e g A_e\sin\theta=\dfrac{\rho_e V^2 D C_{L0}}{4}q \\ \dfrac{\partial^2 q}{\partial t^2}+\varepsilon\Omega_f(q^2-1)\dfrac{\partial q}{\partial t}+{\Omega_f}^2 q=\dfrac{\alpha}{D}\dfrac{\partial^2 z}{\partial t^2} \end{cases} \tag{5}$$

subjected to pinned-pinned boundary conditions:

$$\begin{aligned} &z(0,t)=0\ ,\ \frac{\partial^2 z(0,t)}{\partial x^2}=0\ , \\ &z(\mathrm{L},t)=0\ ,\ \frac{\partial^2 z(L,t)}{\partial x^2}=0 \end{aligned} \tag{6a}$$

and

$$\begin{aligned} &q(0,t)=0\ ,\ \frac{\partial^2 q(0,t)}{\partial x^2}=0\ , \\ &q(\mathrm{L},t)=0\ ,\ \frac{\partial^2 q(\mathrm{L},t)}{\partial x^2}=0 \end{aligned} \tag{6b}$$

By introducing the following dimensionless variables:

$$\begin{aligned} &x^*=\frac{x}{L}\ ,\ z^*=\frac{z}{D}\ ,\ t^*=\frac{t}{L^2}\sqrt{\frac{EI}{m_p}}\ , \\ &U^*=UL\sqrt{\frac{m_p}{EI}}\ ,\ V^*=VL\sqrt{\frac{m_p}{EI}}\ , \\ &\Omega_f{}^*=\Omega_f L^2\sqrt{\frac{m_p}{EI}}\ ,\ \beta=\frac{\rho_e V^{*2} C_{L0} L^2}{4m_p} \end{aligned} \tag{7}$$

the dimensionless coupling system is yielded, where the asterisks are omitted for simplicity:

$$\begin{cases} \dfrac{\partial^4 z}{\partial x^4}+(\dfrac{m_i U^2}{m_p}+\dfrac{PA_iL^2}{EI}-\dfrac{T_aL^2}{EI})\dfrac{\partial^2 z}{\partial x^2}+\dfrac{(m_p+m_i)gL^3\cos\theta}{EI}\dfrac{\partial z}{\partial x}+\dfrac{2m_iU}{m_p}\dfrac{\partial^2 z}{\partial x\partial t} \\ +(r_s+r_f)\dfrac{L^2}{\sqrt{EIm_p}}\dfrac{\partial z}{\partial t}+\dfrac{(m_p+m_i+m_e)}{m_p}\dfrac{\partial^2 z}{\partial t^2}+\dfrac{(m_p+m_i)gL^4\sin\theta}{EID}-\dfrac{\rho_e g A_e \sin\theta L^4}{EID}=\beta q \\ \dfrac{\partial^2 q}{\partial t^2}+\varepsilon\Omega_f(q^2-1)\dfrac{\partial q}{\partial t}+{\Omega_f}^2 q=\alpha\dfrac{\partial^2 z}{\partial t^2} \end{cases} \tag{8a}$$

together with the dimensionless boundary conditions expressed as:

$$\begin{aligned} &z(0,t)=0\ ,\ \frac{\partial^2 z(0,t)}{\partial x^2}=0\ , \\ &z(1,t)=0\ ,\ \frac{\partial^2 z(1,t)}{\partial x^2}=0 \end{aligned} \tag{8b}$$

and

$$\begin{aligned} &q(0,t)=0\ ,\ \frac{\partial^2 q(0,t)}{\partial x^2}=0\ , \\ &q(1,t)=0\ ,\ \frac{\partial^2 q(1,t)}{\partial x^2}=0 \end{aligned} \tag{8c}$$

Besides, a random noise with an amplitude of order $O(10^{-3})$ is applied to the fluid variable q for the initial conditions (Violette, *et al*, 2007):

$$z(x,0)=0\ ,\ \frac{\partial z(x,0)}{\partial t}=0 \tag{9a}$$

and

$$q(x,0)=O(10^{-3})\ ,\ \frac{\partial q(x,0)}{\partial t}=0 \tag{9b}$$

It has to be mentioned that θ is the angle between the pipeline and the direction of gravity, and the slope of the seabed or the inclination angle of the pipeline is assumed to be γ, and $\gamma=\dfrac{\pi}{2}-\theta$.

3. INTEGRAL TRANSFORM SOLUTION

In this section, the coupling system, i.e. the initial- and boundary-value problem given by Equations (8) and (9) are solved through GITT. This method is a semi-analytical method, which is a classical approach for solving heat and fluid flow problems, and can realize controlled accuracy and efficient computational performance (Cotta, 1993; Cotta, 1994; Cotta, 1997 and Cotta, 1998). The application of GITT has been further adopted in the area of structural mechanics (Ma, *et al*, 2006; An & Su, 2011; Matt, 2013a; Matt, 2013b; An & Su, 2014a; and An & Su, 2014b). The implementation of this technique to solve coupled fluid and structure problems has been more frequent over the last few years (Matt, 2009; Gu, *et al*, 2012; Gu, *et al*, 2013a; Gu, *et al*, 2013b; An & Su, 2015; An, *et al*, 2016; Li, *et al*, 2016; and Gu, *et al*, 2016).

The first step in applying GITT is to define the auxiliary eigenvalue problem. For the transverse displacement of a pipeline and the wake variable, the eigenvalue problems are chosen respectively as:

$$\frac{\mathrm{d}^4 X_i(x)}{\mathrm{d}x^4}=\phi_i^4 X_i(x),\ 0<x<1 \tag{10a}$$

$$\frac{\mathrm{d}^4 Y_k(x)}{\mathrm{d}x^4}=\varphi_k^4 Y_k(x),\ 0<x<1 \tag{10b}$$

with the boundary conditions being:

$$\begin{aligned} &X_i(0)=0\ ,\ \frac{\mathrm{d}^2 X_i(0)}{\mathrm{d}x^2}=0\ , \\ &X_i(1)=0\ ,\ \frac{\mathrm{d}^2 X_i(1)}{\mathrm{d}x^2}=0 \end{aligned} \tag{11a}$$

$$\begin{aligned} &Y_k(0)=0\ ,\ \frac{\mathrm{d}^2 Y_k(0)}{\mathrm{d}x^2}=0\ , \\ &Y_k(1)=0\ ,\ \frac{\mathrm{d}^2 Y_k(1)}{\mathrm{d}x^2}=0 \end{aligned} \tag{11b}$$

where X and ϕ_i are the eigenfunction and the eigenvalue of problem Equation (10a); likewise Y_k and φ_k are the eigenfunction and the eigenvalue of problem Equation (10b). The eigenfunctions both satisfy the following orthogonality,

$$\int_0^1 X_i(x)X_j(x)\mathrm{d}x=\delta_{ij}N_i \tag{12a}$$

$$\int_0^1 Y_k(x)Y_l(x)\mathrm{d}x=\delta_{kl}N_k \tag{12b}$$

where δ_{ij} and δ_{kl} is the Kronecker delta. For $i\neq j$, $\delta_{ij}=0$; and for $i=j$, $\delta_{ij}=1$. Likewise, for $k\neq l$, $\delta_{kl}=0$; for $k=l$, $\delta_{kl}=1$.

The normalization integrals are:

$$N_i = \int_0^1 X_i^2(x)\,\mathrm{d}x \tag{13a}$$

$$N_k = \int_0^1 Y_k^2(x)\,\mathrm{d}x \tag{13b}$$

The eigenvalue problems (10a) and (10b) with the boundary conditions (11a) and (11b) are now analytically solved to yield:

$$X_i(x) = \sin(\phi_i x) \tag{14a}$$

$$Y_k(x) = \sin(\varphi_k x) \tag{14b}$$

where the eigenvalue is obtained:

$$\phi_i = i\pi\ ,\quad i = 1,\ 2,\ 3,\ \ldots \tag{15a}$$

$$\varphi_k = k\pi\ ,\quad k = 1,\ 2,\ 3,\ \ldots \tag{15b}$$

And by introducing Equations (14) and (15) to Equation (13), the normalization integrals are evaluated as

$$N_i = \frac{1}{2}\ ,\quad i = 1,\ 2,\ 3,\ \ldots \tag{16a}$$

$$N_k = \frac{1}{2}\ ,\quad k = 1,\ 2,\ 3,\ \ldots \tag{16b}$$

Therefore, in this case, the normalized eigenfunction correlates with the original eigenfunction through the following function:

$$\tilde{X}_i(x) = \frac{X_i(x)}{N_i^{1/2}} \tag{17a}$$

$$\tilde{Y}_k(x) = \frac{Y_k(x)}{N_i^{1/2}} \tag{17b}$$

The next step is to define the integral transform pair – the integral transform itself and the inversion formula. For the transverse displacement of the free span:

$$\bar{z}_i(t) = \int_0^1 \tilde{X}_i(x) z(x,t)\,\mathrm{d}x\ ,\ \text{transform} \tag{18a}$$

$$z(x,t) = \sum_{i=1}^{\infty} \tilde{X}_i(x)\bar{z}_i(t)\ ,\ \text{inversion} \tag{18b}$$

For the wake variable:

$$\bar{q}_k(t) = \int_0^1 \tilde{Y}_k(x) q(x,t)\,\mathrm{d}x\ ,\ \text{transform} \tag{19a}$$

$$q(x,t) = \sum_{k=1}^{\infty} \tilde{Y}_k(x)\bar{q}_k(t)\ ,\ \text{inversion} \tag{19b}$$

The third step is the transformation of the governing partial differential equations into a system of ordinary differential equations with respect to the time t, by employing the definition of $z_i(t)$ and $q_k(t)$ given by Equations (18a) and (19a). By multiplying both sides of equation system (8a) by $\tilde{X}_i(x)$ and $\tilde{Y}_k(x)$ respectively, integrating on x from 0 to 1, and then using Equations (18b) and (19b), the following ordinary differential equation system is yielded:

$$\begin{cases} \phi_i^4 \bar{z}_i(t) + \left(\dfrac{m_i U^2}{m_p} + \dfrac{PA_iL^2}{EI} - \dfrac{T_aL^2}{EI}\right)\displaystyle\sum_{j=1}^{\infty} A_{ij}\bar{z}_j(t) + \dfrac{(m_p+m_i)gL^3\cos\theta}{EI}\sum_{j=1}^{\infty} B_{ij}\bar{z}_j(t) + \dfrac{2m_iU}{m_p}\sum_{j=1}^{\infty} B_{ij}\dfrac{\mathrm{d}\bar{z}_j(t)}{\mathrm{d}t} \\ + \dfrac{(r_s+r_f)L^2}{\sqrt{EIm_p}}\dfrac{\mathrm{d}\bar{z}_j(t)}{\mathrm{d}t} + \dfrac{(m_p+m_i+m_e)}{m_p}\dfrac{\mathrm{d}^2\bar{z}_i(t)}{\mathrm{d}t^2} + C_i\dfrac{(m_p+m_i)gL^4\sin\theta}{EID} - C_i\dfrac{\rho_e g A_e \sin\theta L^4}{EID} = \beta\displaystyle\sum_{k=1}^{\infty} D_{ik}\bar{q}_k(t) \\ \dfrac{\mathrm{d}^2\bar{q}_k(t)}{\mathrm{d}t^2} + \varepsilon w_f \displaystyle\sum_{l=1}^{\infty}\sum_{r=1}^{\infty}\sum_{s=1}^{\infty} E_{klrs}\bar{q}_l(t)\bar{q}_r(t)\dfrac{\mathrm{d}\bar{q}_s(t)}{\mathrm{d}t} - \varepsilon w_f\dfrac{\mathrm{d}\bar{q}_k(t)}{\mathrm{d}t} + {w_f}^2\bar{q}_k(t) = \alpha\displaystyle\sum_{i=1}^{\infty} F_{ki}\dfrac{\mathrm{d}^2\bar{z}_i(t)}{\mathrm{d}t^2} \end{cases} \tag{20a}$$

where the coefficients are analytically determined by the following integrals:

$$A_{ij} = \int_0^1 \tilde{X}_i(x)\frac{\mathrm{d}^2\tilde{X}_j(x)}{\mathrm{d}x^2}\mathrm{d}x\ ,\ B_{ij} = \int_0^1 \tilde{X}_i(x)\frac{\mathrm{d}\tilde{X}_j(x)}{\mathrm{d}x}\mathrm{d}x\ ,$$
$$C_i = \int_0^1 \tilde{X}_i(x)\,\mathrm{d}x\ ,\ D_{ik} = \int_0^1 \tilde{X}_i(x)\tilde{Y}_k(x)\,\mathrm{d}x\ ,$$
$$E_{klrs} = \int_0^1 \tilde{Y}_k(x)\tilde{Y}_l(x)\tilde{Y}_r(x)\tilde{Y}_s(x)\,\mathrm{d}x\ ,\ F_{ki} = \int_0^1 \tilde{Y}_k(x)\tilde{X}_i(x)\,\mathrm{d}x \tag{20b}$$

The initial conditions are also transformed with spatial coordinate being eliminated, yielding

$$\bar{z}_i(0) = 0\ ,\quad \frac{\mathrm{d}\bar{z}_i(0)}{\mathrm{d}t} = 0 \tag{21a}$$

$$\bar{q}_k(0) = \int_0^1 \tilde{Y}_k(x) q(x,0)\,\mathrm{d}x\ ,\quad \frac{\mathrm{d}\bar{q}_k(0)}{\mathrm{d}t} = 0 \tag{21b}$$

For computation efficiency, the expansions for $z(x,t)$

and $q(x,t)$ are both truncated to N orders. When $\bar{z}_i(t)$ and $q_k(t)$ in Equation (20) are numerically evaluated, the inversion formulas Equations (18b) and (19b) are then applied to recover the analytical expressions for the dimensionless $z(x,t)$ and $q(x,t)$.

4. RESULTS AND DISCUSSION

In this section, the semi-analytical results for the transverse displacement $z(x,t)$ of the inclined fluid-transporting submarine pipelines subject to uniform internal flow and external cross flow will be solved through GITT in case studies. The convergence behavior of the GITT solutions is concluded to have a good performance based on the convergence analysis in the literature mentioned previously (An & Su, 2014b; Li, *et al*, 2016). For this reason, the convergence analysis will not be discussed for the present study, and for all the following work the truncation order N = 12 will be used in the case study.

The main geometric and physical properties of submarine pipeline and the fluid in the parametric studies are summarized in Tables 1 and 2. In addition, the reduced velocity $V_r = V/(f_s D)$ is introduced here, where $f_s = \Omega_s/(2\pi)$ is the fundamental natural frequency. The range of the reduced velocity studied in the present paper is within $Vr \in [4, 8]$, corresponding the dimensionless external current velocity range $V \in [0.018, 0.036]$, which is the lock-in region of VIV.

4.1 GRAVITY EFFECT

The existing mathematical model, as shown by Equation (22), for predicting the dynamic response of free-spanning pipelines often ignores the gravity terms (Fyrileiv & Mørk, 2002; Lou, *et al*, 2005), which is the same if the acceleration due to the gravity g is set as zero in Equation (3). However, the proposed structural model Equation (4) in the present paper takes into consideration not only the angle terms but also the gravity terms.

The time history results of the mid-point of a horizontal free-spanning pipeline is calculated with dimensionless U = 0.5, V = 0.03, as shown in Figure 4. It is found that when the gravity terms are ignored, i.e. g = 0, the vibration center of the span mid-point is z = 0; and when the gravity terms are considered, i.e. g = 9.8 m/s^2, the vibration center of the span mid-point deviates to z = -9.7930.

$$EI\frac{\partial^4 z}{\partial x^4} + (m_i U^2 + PA_i - T_a)\frac{\partial^2 z}{\partial x^2} + 2m_i U\frac{\partial^2 z}{\partial x \partial t} + (r_s + r_f)\frac{\partial z}{\partial t} + (m_p + m_i + m_e)\frac{\partial^2 z}{\partial t^2} = F_L \tag{22}$$

Table 1 Geometric and physical properties of submarine pipeline.

D [m]	L [m]	D_i [m]	ρ_p [kg/m^3]	E [Pa]	ζ
0.35	76	0.325	8200	2.0×10^{11}	0.005

Table 2 Physical properties of internal and external fluid.

ρ_i [kg/m^3]	ρ_e [kg/m^3]	C_{D0}	C_M	C_{L0}	St	α	ε
908.2	1025	1.2	1	0.3	0.2	12	0.3

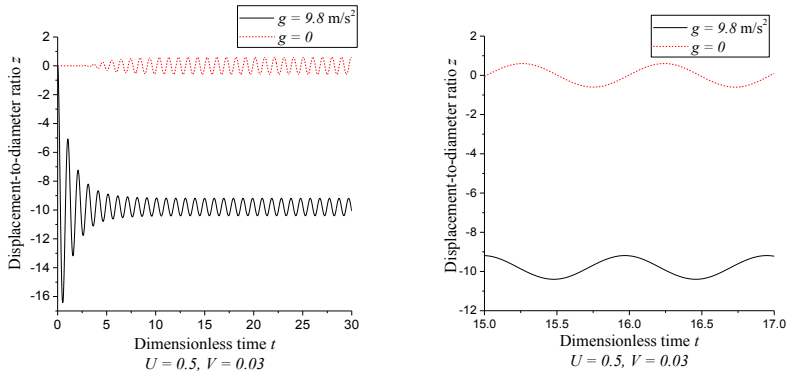

(a) Dimensionless $t \in [0, 30]$ (b) Dimensionless $t \in [15, 17]$

Figure 4: Cross-flow time history of the mid-point of a horizontal free span.

If the time history of the span mid-point which considers the gravity effect (i.e. the black curve) is translated upwards by 9.7930, Figure 5 is plotted. Observation indicates that, for horizontal spans, the gravity effect on the vibration amplitude is very subtle. When gravity is ignored, the maximum displacement-to-diameter ratio is 0.6029; and when gravity is considered, the maximum displacement-to-diameter ratio is 0.6043. The results are very close. The spectral analysis shown in Figure 6 (where PSD refers to power spectral density) also proves that gravity does not affect vibration frequency of the horizontal free-spanning pipeline.

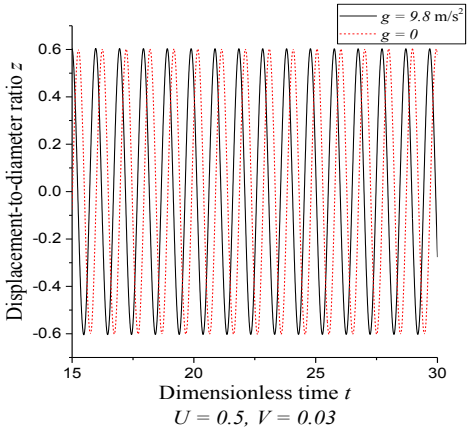

Figure 5: Comparison of the vibration amplitude between horizontal free spans considering gravity and ignoring gravity ($t \in [15,\ 30]$).

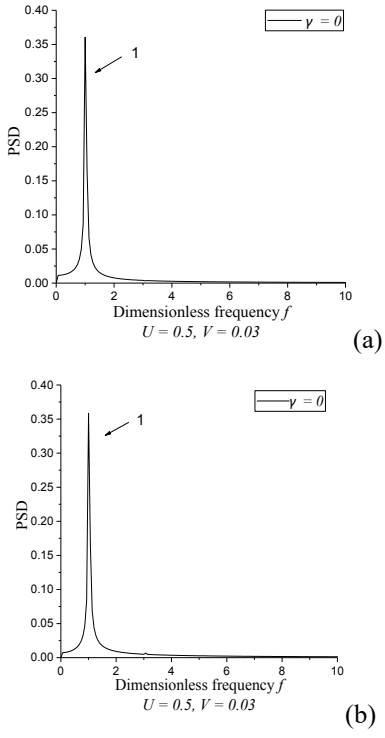

(a) $g = 9.8$ m/s^2
(b) $g = 0$

Figure 6: Frequency analysis of the horizontal free span.

The same comparison is also done for a free span over a 45° slope. The time history results of the mid-point of an inclined free-spanning pipeline is calculated with dimensionless $U = 0.5$, $V = 0.03$, as shown in Figure 7. It is found that when the gravity terms are ignored, i.e. $g = 0$, the vibration center of the span mid-point is $z = 0$; and when the gravity terms are considered, i.e. $g = 9.8$ m/s^2, the vibration center of the span mid-point deviates to $z = -6.8506$.

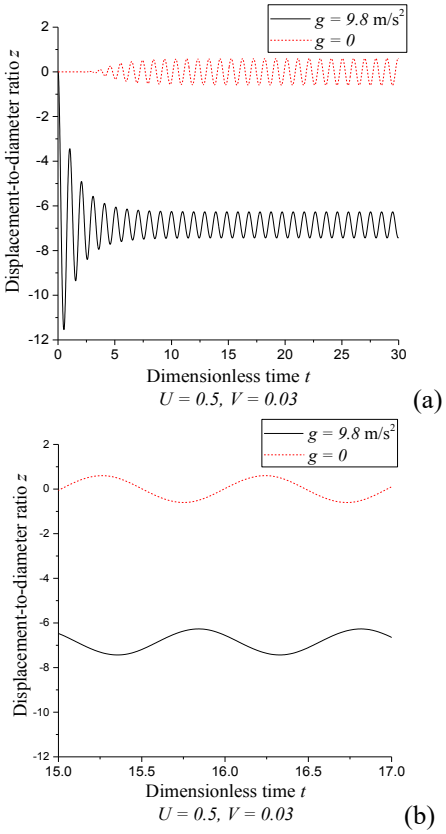

(a) Dimensionless $t \in [0,\ 30]$
(b) Dimensionless $t \in [15,\ 17]$

Figure 7: Cross-flow time history of the mid-point of a free span with a 45° slope.

If the time history of the span mid-point which considers the gravity effect (i.e. the black curve) is translated upwards by 6.8506, Figure 8 is plotted. It can be observed that, for inclined free spans, the gravity effect will change the vibration amplitude of the system. When gravity is ignored, the maximum displacement-to-diameter ratio is 0.6029; and when gravity is considered, the maximum displacement-to-diameter ratio is 0.5823, and the difference is very distinct. The FFT analysis shown in Figure 9 displays that gravity does not affect vibration frequency of the inclined free-spanning pipeline. However, it has to be admitted that the difference in the vibration amplitude cannot be ignored, thus if the free-spanning pipeline system is over seabed slope, the inclination of the free-spanning pipeline has to be considered when predicting the dynamic behaviors of the system.

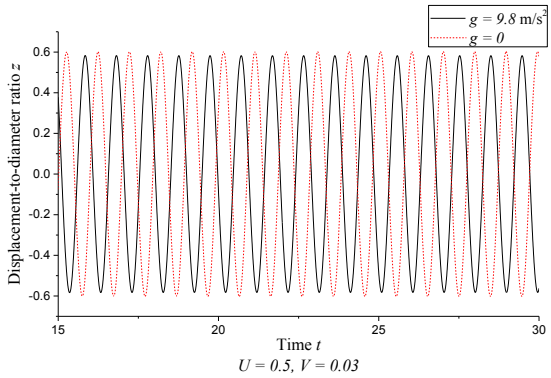

Figure 8: Comparison of the vibration amplitude between the free span with a 45° slope considering gravity and ignoring gravity ($t \in [15, 30]$).

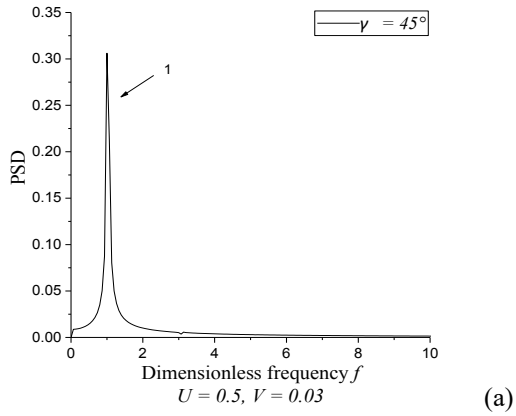

(a) $g = 9.8$ m/s^2

(b) $g = 0$

Figure 9: Frequency analysis of the free span with a 45° slope.

The mode shapes of free-spanning pipelines with $U = 0.8$, $V = 0.035$, and $\gamma = 45°$ are shown in Figure 10, where (a) is depicted when gravity is considered and (b) is depicted when gravity is ignored. The lines are plotted for a time internal of 0.05 during $t \in [15, 16]$. The mode shapes also clearly reveal the difference between the two different cases.

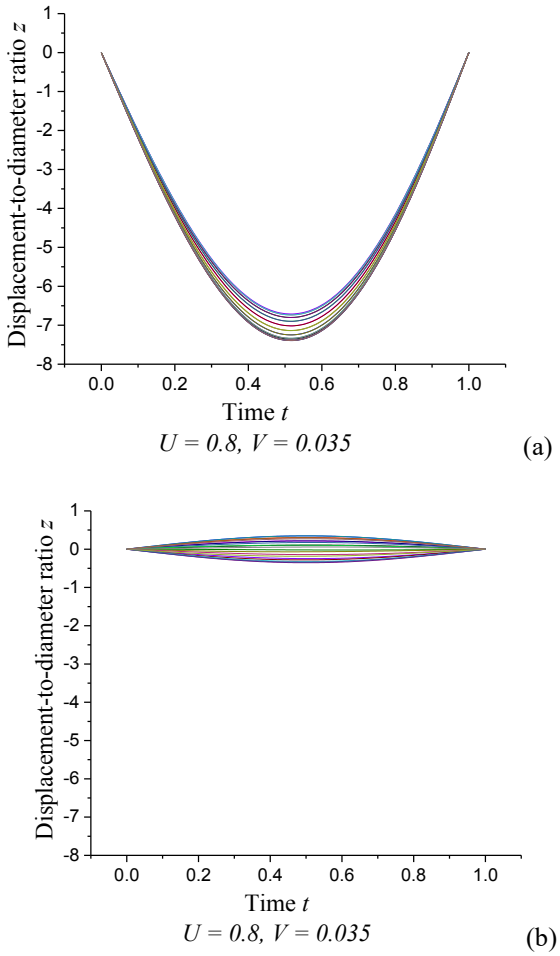

(a) $g = 9.8$ m/s^2

(b) $g = 0$

Figure 10: Instantaneous displacement during $t \in [15, 16]$

4.2 NATURAL FREQUENCY

To calculate the natural frequency of the free-spanning pipeline system using GITT, both the external and internal flow velocities are set as zero. A random noise with an amplitude of order $O(10^{-3})$ is applied to the dimensionless transverse displacement z. Calculations are done respectively for the free-spanning pipeline with a slope angle of 0°, 15°, 30° and 45° respectively. The spectral analysis of the midpoint vibration under the above-mentioned conditions are provided in Figure 11.

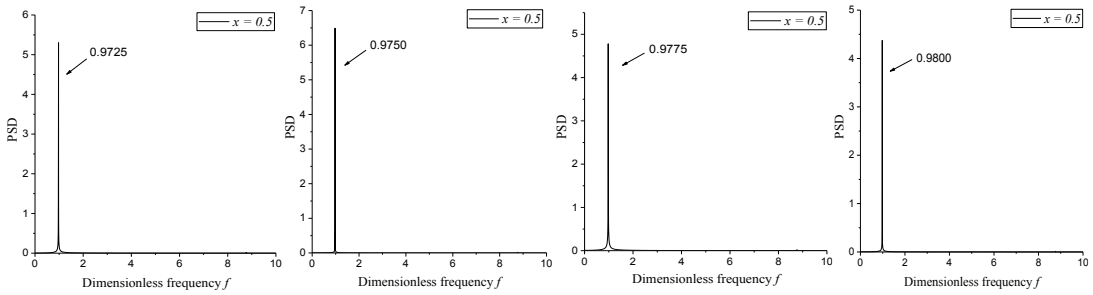

Figure 11: Frequency analysis of the free vibration of free span with different slope angles.

The dominating frequencies shown in Figure 11 (a-d) represents the fundamental natural frequency of the free-spanning pipeline. It can be observed that with the increase in seabed slope, the natural frequency of the free-spanning pipeline will also increase. This can be explained as the slope rises, the axial force will increase due to gravity, hence the natural frequency being increased. The results provided in Figure 10 are non-dimensional, and the natural frequencies in Hz are summarized in Table 3.

Table 3 Effects of the slope angle on the natural frequency of the free spanning pipeline.

Seabed slope γ	**Fundamental natural frequency [Hz]**
0	0.0993
15°	0.0995
30°	0.0997
45°	0.1001

Figure 12 summarizes how the internal flow affects the structural natural frequency. The descending curves in the figure imply that with the increase in internal flow velocity, the structural natural frequency will decline. And when the internal flow velocity is the same, the steeper the seabed slope is, the higher the natural frequency is.

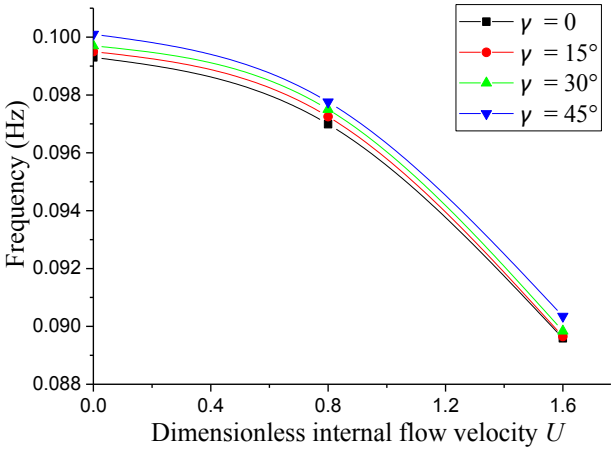

Figure 12: Natural frequency with different slope angles.

4.3 SLOPE EFFECT

Assume the internal flow velocity is zero, the effect of the seabed slope on the vibration amplitude of the free-spanning pipeline system is studied. Results show that when the reduced velocity $Vr \le 6$, the vibration amplitude increases as the slope reduces; when $Vr > 6$, the vibration amplitude increases as the slope increases (as shown in Figure 13). This indicates a shift in the lock-in region as the slope changes. Since the structural natural frequency is increased with the increase of the slope, which has been proved in Section 4.2, the lock-in will occur under higher vortex-shedding frequency, or higher current velocity, for free-spanning crossing the steeper slope.

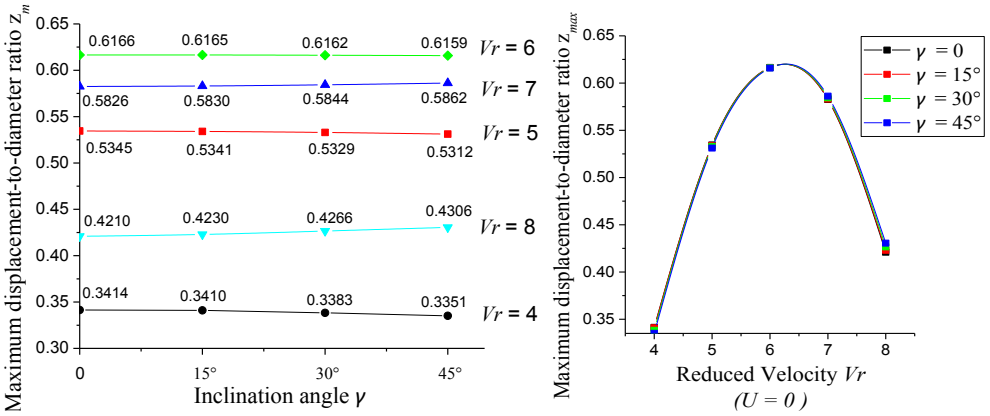

Figure 13: Maximum cross-flow displacement of free span with different slope angles under different current velocity.

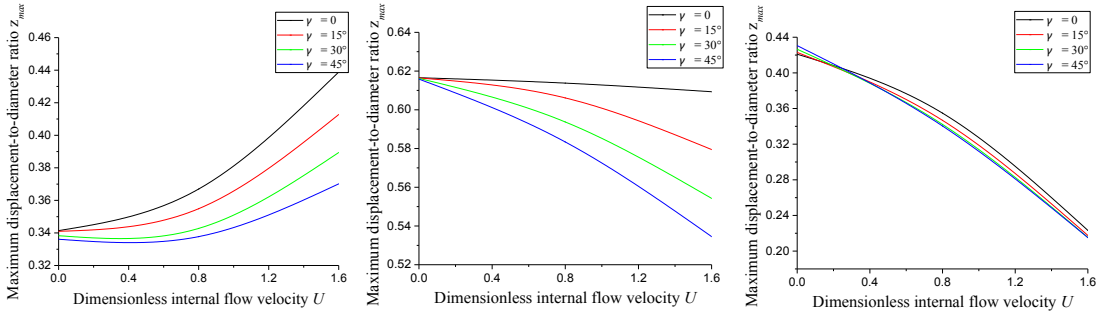

(a) $Vr = 4$ (b) $Vr = 6$ (c) $Vr = 8$

Figure 14: Maximum displacement of free span with different slope angles subject to different internal flow velocity.

When the pipeline is conveying internal fluid, three different reduced velocities, i.e. $Vr = 4, 6, 8$ are chosen for the parametric studies, representing respectively the three stages in VIV lock-in, namely, the lock-in start, the resonation and the lock-in end. The maximum displacement-to-diameter ratios are calculated, and the results are displayed in Figure 14. It is observed that before the resonance happens, the amplitude of vibration increases as the internal flow velocity increases. When the resonance happens, i.e. $Vr = 6$, the effect of internal flow velocity change on the amplitude of vibration is very subtle for the horizontal free span; however, as the seabed slope become steeper, the effect of internal flow velocity change becomes more distinct. When the lock-in finishes, the amplitude of vibration declines as the internal flow velocity increases; and the steeper the slope is, the sharper the declining trend is.

5. CONCLUSION

In the present paper, the mathematical model for the vibration of inclined fluid-transporting free-spanning submarine pipelines is established, and a non-linear wake oscillator is employed to model the vortex shedding behind the pipeline free span. With GITT, the governing equation system of vibration is solved, and the semi-analytical solutions for the transverse displacement is obtained. Hence the conclusion can be summarized as follows:

(1) It is proved that for horizontal free-spanning pipelines, the effect of the gravity can be ignored when predicting the dynamic behaviors; while for inclined free-spanning pipelines, the gravity effect has to be taken into consideration. If the effect of the gravity is ignored for inclined pipelines, the vibration amplitude will be over-estimated.

(2) It is calculated that with the increase in seabed slope, the natural frequency of the free-spanning pipeline will also increase. Besides, with the increase in internal flow velocity, the structural natural frequency will decline. To fully understand the natural frequency of inclined fluid-conveying pipelines provides a reliable guide for pipeline design.

(3) The existence of the internal flow will affect the displacement of the free-spanning pipeline system, while the slope of the seabed will further signify the internal flow effect. As the degree of the slope changes, the VIV lock-in region will also change. Since the increase of the slope will cause a rise in structural natural frequency, the lock-in will occur under a higher vortex-shedding frequency. The accurate prediction of the structural dynamic behaviors and lock-in region is of vital importance for pipeline design and fatigue life prediction.

6. ACKNOWLEDGEMENTS

This work is supported by National Key Research and Development Plan of China (Grant No. 2016YFC0303704), National Natural Science Foundation of China (Grant No. 51509258), National Science and Technology Major Project of China (2016ZX05033-004-004).

7. REFERENCES

1. FYRILEIV, O., MØRK, K. *Structural response of pipeline free spans based on beam theory*. Proceedings of ASME 2002, International Conference on Offshore Mechanics and Arctic Engineering, Norway, June 23-28, 2002, 175-183.
2. VEDELD, K., SOLLUND, H., HELLESLAND, J. *Free vibrations of free spanning offshore pipelines*. *Eng. Struct.* 2013, 56(56): 68-82.
3. FACCHINETTI, M.L., DE LANGRE, E., BIOLLEY, F. *Coupling of structure and wake oscillators in vortex-induced vibrations*. *J. Fluids Struct.* 2004, 19(2), 123-140.
4. LOW, Y.M., SRINIL, N. *VIV fatigue reliability analysis of marine risers with uncertainties in the wake oscillator model*. *Eng. Struct.* 2016, 106, 96-108.
5. GUO, H.Y., LOU, M., DONG, X.L. *Experimental study on vortex-induced vibration of risers transporting fluid*. Proceedings of the 16th International Offshore and Polar Engineering Conference, USA, May 28-June 2, 2006, 820-823.
6. HOUSER, G.W. *Bending vibrations of a pipeline containing flowing fluid*. *J. Appl. Mech.* 1952, 19, 205-208.
7. SHEN, Z.H., ZHAO, Q. *Effects of internal flow on vortex-induced vibration and fatigue life of submarine pipelines*. *China Ocean Eng.* 1996, 10(3), 251-260.
8. GUO, H.Y., WANG, Y.B., FU, Q. *The effect of internal fluid on the response of vortex- induced vibration of marine rises*. *China Ocean Eng.* 2004, 18(1), 11-20.
9. LOU, M., DING, J., GUO, H.Y., DONG X.L. *Effect of internal flow on vortex-induced vibration of submarine free spanning pipelines*. *China Ocean Eng.* 2005, 19, 147-154.
10. GUO, H.Y., LOU, M. *Effect of internal flow on vortex-induced vibration of risers*. *J. Fluids Struct.* 2008, 24(4), 496-504.
11. KAEWUNRUEN, S., CHIRAVATCHRADEJ, J., CHUCHEEPSAKUL, S. *Nonlinear free vibrations of marine risers/pipes transporting fluid*. *Ocean Eng.* 2005, 32(32), 417-440.
12. DAI, H.L., WANG, L., QIAN, Q., NI, Q. *Vortex-induced vibrations of pipes conveying pulsating fluid*. *Ocean Eng*. 2014, 77(2), 12-22.
13. DRAGO, M., MATTIOLI, M., BRUSCHI, R., VITALI, L. *Insights on the design of free-spanning pipelines*. Philos. Trans. R. Soc. London, Ser. *A*. 2015, 373(2033).
14. PAIDOUSSIS, M.P. *Fluid-structure interactions: slender structures and axial flow*. Academic Press, California, 1998.
15. GAN C., JING S., YANG S., LEI H. *Effects of supported angle on stability and dynamical bifurcations of cantilevered pipe conveying fluid*. Appl. Math. Mech. 2015, 36(6), 729-746.
16. JING, S., GAN, C.B., YANG, S.X., LEI, H. *Vibration characteristics of an inclined pinned-pinned fluid-conveying pipe* (in Chinese). Eng. Mech. 2015, 32(12), 243-256.
17. CLOUGH, R.W., PENZIEN, J. *Dynamics of Structures*. McGraw-Hill, Inc. New York, 1975.
18. IWAN, W.D. *The vortex- induced oscillation of non-uniform structural systems*. J. Sound Vib. 1981, 79(2), 291-301.
19. VIOLETTE, R., DE LANGRE, E., SZYDLOWSKI, J. *Computation of vortex-induced vibrations of long structures using a wake oscillator model: Comparison with DNS and experiments*. Comput. Struct. 2007, 85(11-14), 1134-114.
20. COTTA, R.M. *Integral Transforms in Computational Heat and Fluid Flow*. CRC Press, Florida, 1993.
21. COTTA, R.M. *Benchmark results in computational heat and fluid flow: the integral transform method*. J. Heat Mass Transfer. 1994, 37, 381-393.
22. COTTA, R.M., MIKHAILOV, M. D. *Heat Conduction - Lumped Analysis, Integral Transforms, Symbolic Computation*. Wiley/Interscience., London, 1997.
23. COTTA, R.M. *The Integral Transform Method in Thermal and Fluids Science and Engineering*. Begell House, New York, 1998.
24. MA, J.K., SU, J., LU, C.H., LI, J.M. *Integral transform solution of the transverse vibration of an axial moving string*. J. Vib. Meas. Diagn. 2006, 26, 104-107.
25. AN, C., SU, J. *Dynamic response of clamped axially moving beams: Integral transform solution*. Appl. Math. Comput. 2011, 218(2), 249-259.
26. MATT, *C.F.T. Combined classical and generalized integral transform approaches for the analysis of the dynamic behavior of a damaged structure.* Appl. Math. Modell. 2013a, 37(18-19), 8431–8450.
27. MATT, C.F.T. *Simulation of the transverse vibrations of a cantilever beam with an eccentric tip mass in the axial direction using integral transforms*. Appl. Math. Modell. 2013b. 37(22), 9338–9354.

28. AN, C., SU, J. *Dynamic response of axially moving Timoshenko beams: integral transform solution*. Appl. Math. Mech. 2014a, 35(11), 1421-1436.
29. AN, C., SU, J. *Dynamic analysis of axially moving orthotropic plates: Integral transform solution.* Appl. Math. Comput. 2014b, 228, 489-507.
30. MATT, C.F.T. *On the application of generalized integral transform technique to wind-induced vibrations on overhead conductors*. Int. J. Numer. Methods Eng. 2009, 78(8), 901-930.
31. GU, J.J., AN, C., LEVI, C., SU, J. *Prediction of vortex-induced vibration of long flexible cylinders modeled by a coupled nonlinear oscillator: Integral transform solution*. J. Hydrodyn. 2012, 24(6), 888-898.
32. GU, J.J., AN, C., DUAN, M.L., LEVI, C., SU, J. *Integral transform solutions of dynamic response of a clamped-clamped pipe conveying fluid*. Nucl. Eng. Des. 2013a, 254, 237-245.
33. GU, J.J., VITOLA, M., COELHO, J., PINTO, W., DUAN, M.L., LEVI, C. *An experimental investigation by towing tank on VIV of a long flexible cylinder for deepwater riser application*. J. Mar. Sci. Technol. 2013b, 18, 358-369.
34. AN, C., SU, J. *Vibration behavior of marine risers conveying gas-liquid two-phase flow*. Proceedings of the 34th International Conference on Ocean, Offshore and Arctic Engineering, Canada, May 31-June 5, 2015.
35. AN, C., DUAN, M.L., SU, J. *Vibration behavior of pipelines conveying gas-liquid two-phase flow supported on the seabed*. Proceedings of the 35th International Conference on Offshore Mechanics and Arctic Engineering, South Korea, June 19-24, 2016.
36. LI, T.T., LI, X.Z., LIANG, W., SU, J., AN, C., DUAN, M.L. *A semi-analytical solution of the dynamic behavior of free-spanning submarine pipelines conveying fluid*. Proceedings of the 26th International Offshore and Polar Engineering Conference, Greece, June 26-July 1, 2016, 421-426.
37. GU, J.J., MA, T.Q., DUAN, M.L. *Effect of aspect ratio on the dynamic response of a fluid-conveying pipe using the Timoshenko beam model*. Ocean Eng. 2016, 114, 185-191.

